JOINT WMO TECHNICAL PROGRESS REPORT ON THE GLOBAL DATA PROCESSING AND FORECASTING SYSTEM AND NUMERICAL WEATHER PREDICTION RESEARCH ACTIVITIES FOR 2017

Hong Kong Observatory, Hong Kong, China

1 Summary of highlights

(i) The Hong Kong Observatory (HKO) was designated as a Regional Specialized Meteorological Centre (RSMC) for Nowcasting at the 70th Executive Council Meeting of WMO in June 2018. Real-time nowcast products including quantitative precipitation forecast, significant convection and aviation ice-crystal icing are made available to Members on a dedicated website (https://rsmc.hko.gov.hk/nowcast/).

(ii) A collaboration with ECMWF was established to develop the nowcast-NWP blending system using pan European radar nowcast and ECMWF deterministic model and ensemble prediction system (EPS) to support the forecast of heavy precipitation and alert of flooding for the next several hours to few days ahead.

(iii) Com-SWIRLS - the community version of Short-range Warning of Intense Rainstorms in Localized Systems (SWIRLS)" was continuously enhanced in support of the development of rainstorm nowcasting operations at various meteorological services in China, India, Indonesia, Malaysia, Myanmar, the Philippines, South Africa, Thailand and Vietnam.

(iv) The 200-m resolution inner domain of the Aviation Model (AVM) was expanded to provide full coverage of the Hong Kong territory.

(v) An ensemble Kalman filter (EnKF) algorithm was developed for the assimilation of regional weather radar mosaic based on an in-house mesoscale ensemble prediction system (MEPS).

(vi) Extended outlook of the probabilities of daily maximum and minimum temperatures for the next 14 days using post-processed ECMWF EPS forecast, as well as the tropical cyclone track probability map for the next 9 days based on global NWP EPSs were developed and launched to the public.

2 Equipment in use

Machine	Quantity	Peak performance	No. of CPU	Memory	Year of Installation
IBM S814 Server	1	66.9 GFLOPS	4	16 GB	2016
Dell R720 Cluster	1	3.0 TFLOPS (CPU) 9.4 TFLOPS (GPU)	18 CPU 8 GPU	1,728 GB (CPU) 40 GB (GPU)	2014
Dell HPC Cluster	1	18.7 TFLOPS	119	3,504 GB	2013
Dell HPC Cluster	1	19.6 TFLOPS	134	4,288 GB	2013/2016
HP Cluster	1	1.8 TFLOPS (CPU) 15.2 TFLOPS (GPU)	16 CPU 21 GPU	1,056 GB (CPU) 120 GB (GPU)	2012-14
Dell R510 Server	1	68.0 GFLOPS	8	12 GB	2012
IBM BladeCenter JS23	1	64.0 GFLOPS	4	16 GB	2012
Dell R710 Cluster	1	1.3 TFLOPS	16	384 GB	2011[(a)]

[(a)]The operational cluster for the SWIRLS nowcasting system would be decommissioned in 2018 and replaced by a suite of CPU+GPU system with theoretical peak performance of about 40 TFLOPS.

3 Data and Products from GTS in use

The approximate number of bulletins of observations received from GTS (in both alphanumeric and BUFR messages) on a typical day in 2017 is given below:

	Alphanumeric	BUFR
SYNOP/SHIP/BUOY	24,500	8,600
Radiosonde (TEMP/PILOT)	1,500	700
AIREP	650	--
AMDAR	2,600	6,300
SATEM/SATOB	150	1,000
ATOVS	--	2,600
Scatterometer wind (ASCAT)	--	14,500
Wind Profiler	--	260
Drifting Buoy	2,000	--

Other observations and reports, such as RADOB, SAREP and DROPSONDE were also gathered through the GTS during the passage of tropical cyclones.

The approximate number of bulletins or files of NWP products received from GTS on a typical day in 2017 is given below:

Centre	Type	Number
China Meteorological Administration (CMA)	GRIB	130*
Deutscher Wetterdienst (DWD)	GRIB	1,900
European Centre for Medium Range Weather Forecasts (ECMWF)	GRIB	2,300^
Japan Meteorological Agency (JMA)	GRIB	5,500
United Kingdom Meteorological Office (UKMO)	GRIB	2,600

*CMA NWP products are grouped by forecast hour and comprise multiple forecast elements.

^ECMWF stopped the production and transmission of GRIB products at 2.5 degrees since December 2017.

NWP products from the US National Centers for Environmental Prediction (NCEP), ECMWF, JMA, Korea Meteorological Administration (KMA) and Canadian Meteorological Centre (CMC) are also acquired through the Internet.

4 Forecasting system

4.1 System run schedule and forecast ranges

4.1.1 AIR/NHM

The Atmospheric Integrated Rapid-cycle (AIR) forecast model system is operated in two forecast domains with horizontal resolution at 10 km and 2 km (Wong, 2011) using the Non-Hydrostatic Model (NHM) developed by the Japan Meteorological Agency (JMA) (Saito et al. 2006).

The outer 10-km resolution model, named as Meso-NHM, is run 8 times a day to generate 72-hour forecasts. The model domain was in the map projection of Lambert Conformal Conic with the lower left corner at 0.91^{o}N, 84.42^{o}E and the upper right corner at 37.48^{o}N, 168.13^{o}E. The initial condition is based on the 3-dimensional variational data assimilation (3DVAR) analysis at 00, 03, 06, 09, 12, 15, 18 and 21 UTC with observation cut-off time of about 2.5 hours. The boundary conditions are extracted from the ECMWF Integrated Forecast System (IFS) forecasts. Meso-NHM ran in multiple configurations. Details are set out in section 4.3.2.1.

The inner 2-km resolution model, known as RAPIDS-NHM, is run on an hourly basis covering an area 19.5 – 25.0 °N, 111.2 – 117.1 °E with forecast range of 15 hours. The initial condition is obtained from the 3DVAR analysis at 00, 01, …, 23 UTC with observation cut-off time of about 35 minutes, and the boundary conditions are prescribed by Meso-NHM forecasts.

4.1.2 Aviation Model (AVM)

The AVM (Chan and Hon, 2016) is a sub-kilometric implementation of the Weather Research and Forecast (WRF) model (Skamarock, 2008) in support of fine-scale aviation weather forecasts for the HKIA.

AVM is operated in two single-nested forecast domains with horizontal resolution of 600 m and 200 m, covering respectively the Pearl River Estuary region (AVM-PRD) and the whole of Hong Kong including HKIA (AVM-*x*HKA). The outer domain covers an area of about 350 km × 350 km (20.8 – 23.8 °N, 112.2 – 115.6 °E) while the inner domain covers about 110 km x 110 km (22.0 – 22.8 °N, 113.7 – 114.5 °E).

Forecasts of both domains are updated at hourly intervals. The outer AVM-PRD routinely provides T+9 forecasts while the inner AVM-*x*HKA follows an optimised schedule alternating between T+12 and T+3 to provide extra temporal coverage for the HKIA.

Initial conditions are obtained from 3D-VAR analysis performed hourly with observation cut-off time of about 15 minutes. Boundary conditions, as well as first guesses for 3D-VAR analysis, for AVM-PRD and AVM-HKA are based on the latest available output from RAPIDS-NHM and the concurrent forecast of AVM-PRD respectively.

4.2 Medium range forecasting system (4-10 days)

For public consumption, HKO routinely issues two types of medium-range forecast products out to 9 days ahead on Internet website, namely the “9-day Weather Forecast” formulated by forecasters and the computer-generated “Automatic Regional Weather Forecast in Hong Kong & Pearl River Delta Region” (ARWF).

The “9-day Weather Forecast” is formulated primarily based on forecasters’ subjective assessment of observations and various prognostic forecast products from the global models of ECMWF, JMA, NCEP, CMA, KMA and UKMO as well as HKO’s Meso-NHM. Forecast of various meteorological elements are presented to forecasters in various formats, including weather maps, time series, time cross-section, forecast tephigrams, etc. References are also made to other forecast products from the EPSs of ECMWF, JMA and KMA for assessment of the confidence and uncertainty involved.

The ARWF webpage (http://maps.weather.gov.hk/ocf/index_e.html) presents the objective station-specific forecasts and gridded forecasts over Hong Kong and the Pearl River Estuary regions using a web-based geographic information system (GIS). Forecast elements include temperature, relative humidity, wind direction and wind speed, daily chance of rain over Hong Kong, and weather forecast icons. Such forecasts are automatically updated twice a day up to nine days ahead based on the Objective Consensus Forecast methodology. The forecasts are also made available on HKO’s mobile app “MyObservatory”.

4.2.1 Operational techniques for application of NWP products (MOS, PPM, KP, Expert Systems, etc.)

4.2.1.1 In operation

4.2.1.1.1 Tropical Cyclone Information Processing System (TIPS)

The Tropical Cyclone Information Processing System (TIPS) has been in operation since 2005, integrating various information for use by forecasters in the preparation of tropical cyclone forecasts and warnings, including a) NWP products from Meso-NHM operated by HKO (see Section 4.3 below), global models of ECMWF, JMA, UKMO, NCEP, CMA, KMA and CMC, as well as the Hurricane Weather Research and Forecast (HWRF) modelling system of NCEP; b) subjective forecasts and warning from meteorological centres; and c) satellite and radar fixes and imageries from meteorological centres. Ensemble mean tracks from various EPS were also available. TIPS can generate ensemble tracks up to 9 days ahead from deterministic and ensemble mean forecasts for reference by forecasters in formulating the warning tracks.

4.2.1.1.2 Objective Consensus Forecast (OCF)

Post-processing of model outputs from global deterministic models including ECMWF, JMA, NCEP, CMA and UKMO, as well as ECMWF EPS and Meso-NHM (see 4.3) are made using the Objective Consensus Forecast (OCF) method (Engel and Ebert, 2007). Forecast time-series of dry-bulb and wet-bulb temperatures, wind speed and wind direction, dew point, relative humidity and weather icon, as well as daily minimum and maximum temperatures and daily probability of precipitation at various locations in Hong Kong up to 384 hours are generated. In support of assessment on the regional temperatures over Hong Kong in the following 9 days, time-lagged ensembles of the maximum and minimum temperature forecasts from OCF are also made available for forecasters' reference. Wind chill temperature was introduced in 2017 for trial to provide guidance on the impact of wind effect in the perceived temperature condition.

4.2.1.1.3 Automatic Weather Forecast

Automatic Weather Forecast system provides worded/iconified objective forecast guidance in text/icons on local winds, state of sky, weather, temperature and relative humidity up to 9 days ahead for reference by forecasters. It runs twice a day based primarily on 00- and 12-UTC outputs from ECMWF, JMA, NCEP, Meso-NHM, as well as some local forecasting rules. Besides, probabilities of precipitation for each day are computed based on the output of ECMWF EPS. In addition to the use of direct model output, key post-processing techniques employed in the system include linear regression, Kalman–filtering, logistic regression and poor-man's ensemble averaging.

4.2.1.1.4 Analogue Forecast System

In support of forecaster's rainfall forecast, an Analogue Forecast System (AFS) is run based on ECMWF's ERA Interim re-analysis data to capture synoptic characteristics leading to heavy rainfall events in the vicinity of Hong Kong with a higher detection rate and lower false alarm ratio compared to using direct model output in rainfall forecast. AFS guidance is updated once a day based on 12-UTC run of ECMWF model forecast to generate daily rainfall category out to 9 days ahead.

4.2.1.1.5 Tropical Cyclone Forecast Guidance

The EPS tropical cyclone (TC) forecast product suite provides various plots of ensemble tracks and strike probability maps (SPM) based on individual global EPSs, namely ECMWF, NCEP, UKMO, JMA, CMA, KMA and CMC, as well as two grand ensembles (ECMWF + NCEP + UKMO and ECMWF + NCEP + UKMO + JMA). The SPMs represent uncertainties in forecast TC positions up to T+240 hours. An interactive webpage is available for forecasters to generate TC forecast products from ECMWF ensemble tracks during pre-genesis stage.

The statistical-dynamical TC intensity forecast (TINT) guidance makes use of HKO best track data and selected parameters identified from ECMWF's ERA Interim re-analysis to provide objective forecast of TC intensity change in the next 5 days. Another TC forecast guidance namely TINT-RI provides the probability of rapid intensification (RI) up to T+48 hours using 200hPa divergence, 300-500hPa RH, 200-850 hPa vertical wind shear from ECMWF model forecasts and NOAA's tropical cyclone heat potential as predictors. Verification for TCs in 2016-2017 showed that TINT-RI performed more favourably than global NWPs and demonstrated higher skill than HWRF in short-range forecast of RI.

4.2.1.2 Research performed in this field

(a) A multivariate Kalman filter post-processing model was developed to enhance OCF for hill-top temperatures and reduce substantial cold bias in daily maximum temperature under fine weather situation. The new scheme showed that the accuracies of daily minimum and maximum temperature forecasts could be increased by 5-10% after incorporating model forecasts of wind speed, wind direction, relative humidity and cloud amount.
(b) OCF was extended to develop automatic weather forecasts for global major cities and airports. Enhancement of model post-processing system was made to handle temperature adjustment due to complex terrain.

(c) A study to enhance TINT-RI was conducted by incorporating NOAA's high-resolution real-time sea-surface temperature analysis and its anomaly as additional predictors. Results showed that the new model can better capture RI of TCs in South China Sea such as Super Typhoon Hato.

4.2.2 Ensemble Prediction System (EPS)

4.2.2.1 Operationally available EPS products

(a) Meteograms from the EPS of ECMWF, JMA and KMA for the grid points in the vicinity of Hong Kong are generated for forecasters' reference. Other ECMWF EPS products, such as Extreme Forecast Index (EFI), Shift of Tails (SOT), probability of precipitation, probability of high winds, spaghetti diagrams and stamp maps of MSLP and geopotential height at 500hPa level, are also available.
(b) ECMWF EPS diagnostic products are generated for forecasters' assessment on the occurrence of significant convective weather from ingredient-based approach. The probability of thunderstorm (PoTS) and consensus diagnostics of low-level moisture transport, moisture flux convergence and advection of equivalent potential temperature are produced using outputs from all 51 ensemble members.
(c) Ensemble model output statistics (EMOS) has been implemented to post-process ECMWF EPS outputs. Based on the non-homogeneous Gaussian regression, the probabilistic daily minimum and maximum temperature forecasts for the next 14 days are generated from 12 UTC EPS run and made available on HKO website.
(d) An in-house mesoscale ensemble prediction system (MEPS) provides twice-daily (initialised at 00 UTC and 12 UTC) 20-member forecasts up to T+72 for the southern China and western North Pacific region. Post-processed products available in real-time include stamp maps of rainfall and simulated satellite imagery, probabilities of various high-impact weather (including precipitation, high winds, extreme temperatures, instability indices, etc.) as well as tropical cyclone strike probability.

4.2.2.2 Research performed in this field

Non-homogeneous Gaussian regression was extended to post-process other EPS forecast elements such as sea level pressure and wind speed. Other EMOS algorithms to improve probabilistic rainfall forecasts and use of machine learning techniques would be studied to enhance the application of EPS products in forecast of extreme weather.

4.3 Short-range forecasting system (0-72 hrs)

4.3.1 Data assimilation, objective analysis and initialization

4.3.1.1 In operation

4.3.1.1.1 AIR/NHM

Meteorological data assimilated by the 3-dimensional variational data assimilation system (3DVAR) of AIR/NHM are as follows:

(A) From GTS

SYNOP, BUOY, SHIP	surface and ship data
TEMP, PILOT	radiosonde and pilot data
AMDAR and AIREP	aircraft data
ATOVS	retrieved temperature profile from polar-orbiting satellites
AMV	atmospheric motion vector from HIMAWARI-8
Ocean surface wind	scatterometer wind retrieval data from ASCAT/RapidScat/HY-2A
IASI	temperature and humidity retrieval profile data from EUMETSAT Metop IASI (Infrared Atmospheric Sounding Interferometer)
Himawari-8	Clear sky radiance products

(B) <u>Through regional data exchange</u>
Data from automatic weather stations and weather radars in Guangdong

(C) Local observations
Automatic weather station data
Doppler weather radar data
Retrieved wind data from mosaic of weather radars in Hong Kong and Guangdong
Wind profiler data
Ground-based Global Positioning System (GPS) reception network

Initial conditions of Meso-NHM and RAPIDS-NHM are generated using 3DVAR analysis running at full horizontal resolution and model vertical levels. The first guess of 3DVAR analysis in Meso-NHM is obtained from the ECMWF IFS. In RAPIDS-NHM 3DVAR system, the Meso-NHM forecast is used as the background.

Total precipitable water vapour (PWV) retrieved from SSM/I is assimilated in Meso-NHM 3DVAR. To prescribe the sea-surface temperature field in Meso-NHM, SST analysis from ECMWF is used.

In RAPIDS-NHM, PWV from the local ground-based GPS stations and Doppler velocity data from the two weather radars in Hong Kong are assimilated in the 3DVAR analysis. 3-dimensional variational wind retrieval is applied to generate upper level wind data over Hong Kong and nearby regions using Doppler velocity and reflectivity data from the weather radars in Hong Kong and Guangdong. The retrieved wind data are used to support the monitoring and nowcast of severe weather, and they are ingested in RAPIDS-NHM 3DVAR as additional upper-air wind observations (Wong *et al.* 2011).

RAPIDS-NHM 3DVAR is used to provide the hourly mesoscale analysis of wind, temperature, relative humidity on surface and upper levels at full horizontal resolution (2 km). Diagnostic fields including instability indices, equivalent potential temperature, moisture transport and moisture flux convergence are generated for forecasters' reference on analysis of mesoscale weather process and nowcasting of severe weather systems.

4.3.1.1.2 AVM

Meteorological data assimilated by the 3-dimensional variational data assimilation system (3DVAR) of AVM are as follows:

(A) From GTS

SYNOP, BUOY, SHIP	surface and ship data
TEMP, PILOT	radiosonde and pilot data
AMDAR and AIREP	aircraft data

(B) Local observations
Dense surface observations from the automatic weather station networks from Hong Kong and Guangdong, including weather buoys
Wind observations from wind profilers in Hong Kong
Temperature and humidity profiles from microwave radiometer

Initial conditions of AVM-PRD and AVM-*x*HKA are generated using 3D-VAR analysis running at full horizontal resolution and model vertical levels with adjusted increment length scales. The first guess of 3D-VAR analysis in AVM-PRD is based on the output from the latest available run of the 2-km RAPIDS-NHM, normally at a time lag of 1 – 2 hours. For AVM-*x*HKA, the background field is taken from the concurrent AVM-PRD output with outstanding forecast hours, if any, supplemented by Rapids-NHM.

4.3.1.2 Research performed in this field

4.3.1.2.1 RAPIDS-NHM

Research was carried out to study the impact of i) extension of domain; ii) assimilating the clear sky radiance (CSR) from Himawari-8; and iii) assimilation of additional radar data over Southern China. Some positive impact was observed.

4.3.1.2.2 AVM

The blending of upper-air moisture fields (including various hydrometeors) from a combination of global and regional models is being studied with a view to alleviating the deficiency of low clouds occasionally observed in the 200-m AVM-*x*HKA model runs.

4.3.1.2.3 Dropsonde

Following commencement of operation of HKO's dropsonde reconnaissance programme over the South China Sea region, research is being conducted in the assimilation of dropsonde observation profiles (including winds, temperature and humidity) into NWP models for improving the analysis and prediction of TC track, structure and intensity (Chan et al, 2018)

4.3.2 Model

4.3.2.1 In operation

4.3.2.1.1 AIR/NHM

Specification of Meso-NHM and RAPIDS-NHM in AIR forecast model system:

	Meso-NHM	**RAPIDS-NHM**
Horizontal resolution	10 km	2 km
Horizontal grid	Arakawa-C	
Map projection	Lambert Conformal Conic	Mercator
No. of grid points	841x515	305x305
Vertical coordinates	Terrain following height coordinates using Lorenz grid	
No. of vertical levels	50	60
Time step	30 s	8 s
Initial time	00, 03, 06,…, 21 UTC (for using EC Tiedtke based (HKO version) convection scheme) 00 and 12 UTC (for using Kain-Fritsch convection scheme (JMA version))	Every hour
Forecast range	72 hours	15 hours
Initial condition	3DVAR using background from ECMWF IFS forecast	3DVAR using background from Meso-NHM forecast
Boundary condition	ECMWF IFS forecast data (00 and 12 UTC) at 0.125 degree resolution in lat/lon Boundary data including: pressure, horizontal wind components (U and V), temperature (T) and relative humidity (RH) on surface; and U,V,T,RH and geopotential height at 21 pressure levels (1000,975,950,925,900,850,800, 700,600,500,400,300,250,200,150,100, 70, 50, 30, 20, 10 hPa) Boundary data including: pressure, horizontal wind components (U and V), temperature (T) and relative	Meso-NHM forecast on 50 model levels

	humidity (RH) on surface; and U,V,T,RH and geopotential height at 21 pressure levels (1000,975,950,925,900,850,800, 700,600,500,400,300,250,200,150,100, 70, 50, 30, 20, 10 hPa)	
Nesting configuration	One-way nesting	
Topography	USGS GTOPO30 (30 second data smoothed to 1.5 times horizontal resolution) with modifications over Hong Kong areas based on USGS-SRTM (Shuttle Radar Topography Mission) dataset	
Land-use characteristics	USGS Global Land Cover Characterization (GLCC) 30 second data and 24 land-use types with modifications over Hong Kong	
Dynamics	Fully compressible non-hydrostatic governing equations solved by time-splitting horizontal-explicit-vertical-implicit (HEVI) scheme using 4^{th}-order centred finite differencing in flux form	
Cloud microphysics	3-ice bulk microphysics scheme	
Convective parameterization	Kain-Fritsch scheme (JMA version) / EC Tiedtke based scheme (HKO version)	-
Surface process	Flux and bulk coefficients: Over land: Beljaars and Holtslag (1991), Donelan *et al.* (2004); Over sea: Beljaars and Holtslag (1991), Donelan *et al.* (2004) (Meso-NHM (KF scheme) and RAPIDS-NHM); Wong et. al. (2011) (Meso-NHM (EC convection scheme)) Roughness length: Beljaars (1995) and Fairall *et al.* (2003); Stomatal resistance and temporal change of wetness included; 4-layer soil model to predict ground temperature and surface heat flux.	
Turbulence closure model and planetary boundary layer process	Mellor-Yamada-Nakanishi-Niino Level 3 (MYNN-3) (RAPIDS-NHM) / Mellor-Yamada-Nakanishi-Niino Level 2.5 (MYNN-2.5) (Meso-NHM) (Nakanishi and Niino, 2004) with partial condensation scheme (PCS) and implicit vertical turbulent solver Height of PBL calculated from virtual potential temperature profile	
Atmospheric radiation	Long wave radiation process following Kitagawa (2000) Short wave radiation process using Yabu *et al.* (2005) Prognostic surface temperature included; Cloud fraction determined from PCS.	

For further details on NHM and AIR forecast model system, please refer to Saito *et al.* (2006) and Wong (2011) respectively.

4.3.2.1.2 AVM

The characteristics of AVM are shown as follows:

	AVM-PRD	**AVM-*x*HKA**
Horizontal resolution	600 m	200 m
Horizontal grid	Arakawa-C	
Map projection	Mercator	
No. of grid points	581×581	581×581
Vertical coordinates	Terrain-following eta coordinates	
No. of vertical levels	42	55
Initial time	Every hour	
Forecast range	7 - 9 hours	3 - 12 hours
Initial condition	3D-Var using background from RAPIDS-NHM forecast	3D-Var using background from AVM-PRD forecast

Boundary condition	Latest available RAPIDS-NHM forecast interpolated onto 42 pressure levels	Concurrent AVM-PRD forecast on full model levels
Nesting configuration	One-way nesting	
Topography	USGS GTOPO30 (30 second data) with local adaptations	
Land-use characteristics	USGS Global Land Cover Characterization (GLCC) 30 second data and 24 land-use types with local adaptations	
Dynamics	Fully compressible non-hydrostatic governing equations in flux form	
Cloud microphysics	WRF double-moment 6-class scheme	
Convective parameterization	-	
Surface processes and boundary layer	Noah LSM	Smagorinsky-like scheme with local adaptations
Atmospheric radiation	Longwave radiation: RRTMG scheme Shortwave radiation: RRTMG shortwave scheme	

Please refer to Skamarock (2008) and Chan and Hon (2016) respectively for technical details of the Weather Research and Forecast (WRF) Model (Version 3.9.1), and the AVM.

4.3.2.2 Research performed in this field

The feasibility of frequently output (up to 1-minute intervals) wind and temperature predictions by AVM-*x*HKA was studied (Hon and Chan, 2017) with a view to supporting advanced aviation applications in future.

In support of regional aviation hazard predictions under the Asian Aviation Meteorological Centre (AAMC) initiative, an extended-domain limited-area prediction system based on WRF-ARW was being developed to provide short-term aviation-specific forecasts for the area (20°S – 60°N, 45°E – 160°E).

4.3.3 Operationally available NWP products

4.3.3.1 AIR/NHM

For Meso-NHM, 3-hourly prognostic charts on surface (3-hour accumulated rainfall, mean sea level pressure, temperature, relative humidity, wind, CAPE) and upper levels (925, 850, 700, 500 and 200 hPa for elements including geopotential height, wind, relative humidity, divergence, relative vorticity), time series, time cross section, vertical cross section and tephigram for grid points at strategic locations in Hong Kong are generated every 3 hours. For RAPIDS-NHM, similar products are generated but at hourly intervals and hourly output frequency. In 2014, new simulated radar reflectivity products such as maximum reflectivity, reflectivity at 3 km altitude, isothermal reflectivity at -10°C and vertically integrated ice content; as well as the mesoscale diagnostic products including moisture transport, moisture flux convergence and updraft helicity for RAPIDS-NHM were added for forecasters' reference in significant convection forecasting.

4.3.3.2 AVM

Routinely available products from AVM-PRD include prognostic charts of upper-air (wind, humidity, divergence and vorticity) and surface elements (pressure, temperature, dew point and relative humidity) at hourly intervals. Upper-air charts are provided at standard pressure levels of 925, 850, 700, 500 and 200 hPa.

A suite of mesoscale diagnostic parameters (including CAPE, K-Index, vertical windshear and storm-relative helicity) has been developed in support of short-term forecasts of severe convection.

Simulated 3-km radar reflectivity images and simulated cloudy infrared radiances at 600-m horizontal resolution are also routinely generated to provide guidance on mode of convection and regional cloud cover.

Specialised products for aviation applications are mentioned in Section 4.3.4.1.2.

4.3.3.3 Products for other meteorological services

TC track forecast guidance from Meso-NHM is routinely generated and disseminated via GTS. The guidance is issued and updated twice a day based on the 00 and 12 UTC model runs whenever a TC reaching tropical depression strength occurs in the area of responsibility of HKO (10 – 30 ^{o}N, 105 – 125 ^{o}E). The information provided in the guidance includes forecast TC positions and intensity changes at 6-hourly intervals up to 72 hours ahead. TC warning position and intensity analysed by HKO at 00 and 12 UTC are also included as initial values.

Up to the end of 2017, HKO is providing city-specific forecast times series and time cross sections for a total of 188 cities of the RA II Members under the RA II Project on City-Specific NWP Products, via a password-protected web site maintained by HKO. The products are generated using the direct model output from Meso-NHM. Table 4.3.3.1 summarised the forecast elements provided in the RA II project.

Table 4.3.3.1 Forecast of meteorological elements provided in the RA II project on City-Specific NWP Products

Content	Levels	Initial Time	Forecast Hours	Display Format
Sea level pressure	Sea level	00 and 12 UTC	3-hourly intervals from 3 to 72 hours	Graphical and tabulated data formats
3-hourly precipitation	Surface			
Surface relative humidity	Surface			
Total cloud amount	-			
Air temperature	Surface, 925, 850, 700, 600, 500, 400, 300, 250, 200, 150 and 100 hPa			
Dew point temperature				
Wind speed and direction				
Geopotential height	500 hPa			

Selected model products derived from Meso-NHM are also disseminated in graphical format via the Internet (Table 4.3.3.2) for reference by RA II Members under the Asian Consortium for NWP Forecast initiative (URL: http://acnf.weather.gov.hk) as well as public consumption (URL: http://www.weather.gov.hk/nhm/nhme.htm).

Table 4.3.3.2 Meso-NHM-based model forecast charts available on the Internet

Levels	Content	Initial Time	Forecast Hours	Area
Surface	Simulated IR imageries overlaid with rain areas	00, 06, 12 and 18 UTC	06, 12, 18, …72	8 – 46.5 °N, 85 – 148 °E
	Air temperature		00, 06, 12, …72	
	Mean sea level pressure			
	Wind			

	Relative humidity and streamline			
850 hPa	Wind			
	Relative vorticity and streamline			
700 hPa	Wind			
	Relative humidity and streamline			
500 hPa	Wind			
	Geopotential height			
200 hPa	Wind			
	Jet stream and streamline			

4.3.3.4 Products from global models

Forecast products based on the global models from ECMWF, JMA, NCEP, UKMO, CMA and KMA were presented to the forecasters in higher temporal resolution (down to 3-hourly intervals generally and down to 1-hourly intervals for zoom-in surface charts for NCEP) over the first 3- to 5-day of the forecast range.

3-hourly prognostic charts for aviation turbulence, icing and convection are generated every 12 hours. Turbulence and icing products are available at 9 vertical levels from 600hPa to 70 hPa.

4.3.4 Operational techniques for application of NWP products

4.3.4.1 In operation

4.3.4.1.1 AIR/NHM

Post-processed maximum and minimum temperatures from Meso-NHM based on Kalman filtering and linear regression for various locations in Hong Kong were routinely generated for reference of the forecasters.

A vortex tracker specially designed to work on the high resolution model outputs of Meso-NHM is in operation. Taking the mean sea level pressure field and circulation at 850 hPa as inputs, the vortex tracker can effectively distinguish between lee lows and tropical cyclones from the high resolution model outputs of Meso-NHM.

A tropical cyclone forecasting tool called Meso-NHM TC Nowcast was in operation. By extrapolating the movement of the tropical cyclone vortex extracted from Meso-NHM along the warning track, forecast time series of wind strength and pressure at various locations in Hong Kong are produced to facilitate forecasters' assessment of the risk of occurrence of strong and gale force winds over the territory in the next 24 hours.

A TC structure forecasting tool based on the outputs from Meso-NHM was developed. It provides the predicted evolution of various TC wind radii, presented in both textual and graphical formats for the ease of user digestion.

Time-lagged ensemble QPF products were developed using rainfall forecasts from successive runs of Meso-NHM and RAPIDS-NHM. In each NHM domain, direct model output of QPF at a given forecast time from all available model runs were combined to generate gridded time-lagged ensemble rainfall. Forecast rainfall maps of the ensemble mean and 75^{th}-percentile were generated where the latter showed an improved skill over individual runs when verified against gridded quantitative precipitation estimates (QPE) using satellite or radar data.

4.3.4.1.2 AVM

In support of short-term aviation weather forecasts for HKIA, a novel suite of aviation-specific products was developed taking advantage of the very high spatial resolution of the inner AVM-*x*HKA domain. These include (i) forecast potential of significant low-level windshear for each arrival and departure runway corridor; and (ii) forecast spatial distribution of low-level turbulence intensity around HKIA as represented by the eddy dissipation rate (EDR).

Simulated infrared cloudy radiances at 600-m horizontal resolution using AVM-PRD output were generated at high frequency of every 10 minutes and provided useful guidance for diagnosing timing of weather features as well as evaluating model performance in real-time.

4.3.4.1.3 Significant Convection Forecast Products in support of Air Traffic Management

Significant convection forecasts up to 12 hours over key air traffic control areas of the Hong Kong Flight Information Region (HKFIR) are provided at 3-hourly intervals in support of air traffic management (ATM) (Cheung and Lam 2011a). The latest product generation algorithm uses 75 percentile QPF value from ECMWF EPS model output as basis with modifications by aviation weather forecasters.

Blending radar-based extrapolation nowcast with phase-adjusted model QPF from RAPIDS-NHM was implemented for the airspace within 128km from Hong Kong. Blended forecasts were used to generate 6-hour forecasts of significant convection over selected critical Air Traffic Control (ATC) regions including 20 nautical miles of HKIA and the closest holding areas for arrival flights. The product was provided together with the 12-hour significant convection forecast above to support airport operations, as well as the airport and airspace capacity forecasts by local ATC.

4.3.4.1.4 Others

Utilizing global and regional NWP model outputs, a post-processing algorithm is used to produce site-specific objective consensus total cloud cover forecast. The algorithm employs downscaling and model output statistics weighting techniques. The cloud cover forecast is ingested into an empirical sea breeze forecast model used at the Hong Kong International Airport and it improves the accuracy of sea breeze forecast with higher detection rate and lower false alarm ratio.

Probability forecasts of wind speed and crosswind at HKIA exceeding pre-defined thresholds for up to 36 hours ahead during TC situations, generated using the ECMWF EPS (Cheung and Lam 2011b), continued under trial operation to support aviation users in risk assessment for flight planning. To facilitate user interpretation of uncertainty information, the wind forecasts were accompanied by probabilistic forecasts of tropical cyclone distance from HKIA.

4.3.4.2 Research performed in this field

The simulation of infrared and visible cloudy radiances at an unprecedented 200-m horizontal resolution using AVM output was studied and demonstrated feasible (Hon, 2018). Large-area simulated cloudy infrared radiance products were also being developed based on output from the extended-domain regional prediction system (covering 20°S – 60°N, 45°E – 160°E) in support of the AAMC initiative.

An in-house developed, ingredient-based post-processing algorithm that generates thunderstorm potentials based on ECMWF EPS output was proven to have provided useful guidance to aviation forecasters in a number of cases. It was being tested for auto-generation of first guess for the 12-hr significant convection forecast product for air traffic management.

Development was carried out to compare the performance of various turbulence indices forecast derived from ECMWF IFS forecast with turbulence events recorded by QAR flight data. Data from around 200 flights between mid-2015 and late-2016 was used in the study.

4.3.5 Ensemble Prediction System

4.3.5.1 Research performed in this field

An in-house 20-member mesoscale ensemble prediction system (MEPS) based on dynamical downscaling of NCEP GEFS output using the WRF model at a horizontal resolution of 10 km continued to provide real-time probabilistic forecast guidance up to 3 days ahead (Hon, 2015). A suite of probabilistic forecast products were developed and made available for forecasters' reference including exceedance probabilities of rainfall, wind speed and temperature, as well as tropical cyclone strike probability. The MEPS provided useful indication of severe weather along the South China coastal areas, particularly for tropical cyclones and rainstorm cases (Hon and Hon, 2016).

To support assessment of possible alternative scenarios, the MEPS provides stamp map products of hourly/3-hourly rainfall distribution as well as simulated cloudy infrared radiances using RTTOV (Song, Lee and Hon, 2017).

Following the methodology Synder and Zhang (2003), an in-house ensemble Kalman filter (EnKF) algorithm was developed for the assimilation of regional radar reflectivity composites using the MEPS (Chiu and Hon, 2018).

4.4 Nowcasting and Very Short-range Forecasting Systems (0-12 hrs)

4.4.1 Nowcasting system

4.4.1.1 In operation

A trial website of the Regional Specialized Meteorological Centre (RSMC) for Nowcasting of HKO (https://rsmc.hko.gov.hk/nowcast/) was established to provide rapid-update products from a suite of nowcasting systems in support of forecasting and alerting high-impact weather at different spatial and temporal scales for the public, aviation community and international users. A community version of its nowcasting system (Com-SWIRLS) is also available from the RSMC for Nowcasting website to promote knowledge exchange in radar nowcasting techniques and for wider application of nowcasting system. The technical information of the HKO nowcasting systems are summarized in the following sections.

4.4.1.1.1 SWIRLS

SWIRLS (Short-range Warning of Intense Rainstorms in Localized Systems) is a radar-based multi-functional nowcasting system in support of forecast and warning of rainstorms, floods, landslips, thunderstorms, hail and gust (Li *et al.* 2014). Major products of SWIRLS include:

(i) Quantitative Precipitation Estimates (QPE), based on radar, rain gauges and a blending of both by co-Kriging analyses (Yeung *et al*. 2010; Yeung *et al*. 2011).
(ii) Quantitative Precipitation Forecast (QPF) by variational optical flow and extrapolation of radar echoes up to 6-9 hours (Woo and Wong, 2017);
(iii) Nowcast of thunderstorm, hail and gust based on radar signatures and model analyses;
(iv) Probabilistic Quantitative Precipitation Nowcast (PQPN) based on "SWIRLS Ensemble Rainfall Nowcast (SERN)" with a total of 36 members;
(v) Satellite-based nowcast using Himawari-8 data where reflectivity retrieved from H-8 imager data and neural network are blended with radar nowcast to extend the coverage of QPF;
(vi) Automatic guidance for supporting rainstorm warning operations: "Automatic Rainstorm Related Objective Warnings (ARROW)", "SWIRLS Integrated Panel (SIP)" and "SWIRLS Time-series And Mapped Probabilities (STAMP)" for integrated display, and "Special Tips on Intense Rainfall (STIR)" for generating text-based rainfall report and forecast;
(vii) Location-specific rainfall and lightning nowcast for the public and special users through HKO website and mobile apps; and
(viii) Real-time verification system.

4.4.1.1.2 ATNS

The Aviation Thunderstorm Nowcasting System (ATNS) (Li 2009) is used to provide thunderstorm nowcasting products for HKIA and HKFIR. Tracking algorithm is based on TREC, and semi-Lagrangian advection scheme is used to generate the forecast radar reflectivity field. Time series on the severity of the forecast reflectivity in 6-minute interval at strategic locations (air traffic control "way-points") up to the next hour are also generated. Users from ATM and airlines could make reference to the storm severity at various way-points from a web-based display integrating GIS information, forecast reflectivity distribution and the aforementioned time series products. "Amber" and "Red" alerts that correspond to radar reflectivity exceeding 31 dBZ and 41 dBZ respectively affecting the way-points are also provided on the web display. It generates the significant convection for arrival/departure corridors in the next 1 hour and was aimed for use by air traffic control to assess weather impact to traffic flow rate.

4.4.1.1.3 Airport Thunderstorm and Lightning Alerting System (ATLAS)

ATLAS provides cloud-to-ground (C-G) lightning alerts over HKIA for the protection of the personnel working on apron based on actual lightning strikes recorded by the lightning detection systems, as well as forecast lightning by storm tracking algorithm (TREC) and time-lag-ensemble storm tracking method (Li and Lau, 2008). When cloud-to-ground lightning was detected within 16km from the airport, ground operators will be alerted to switch to Bluetooth headsets - Wireless Headset Procedure. "Amber" alert will be issued if cloud-to-ground lightning with intense radar echo is detected within 10km or predicted within 5 km from the centre of the airport. Separate "Red" alerts will be issued for zone A (comprising the passenger and cargo terminal) and zone B (the rest of the airport island) when C-G lightning occurs or is predicted to occur within 1 km of the zones.

ATLAS switched to use data from the enhanced Lightning Location Information System (LLIS) operated by HKO in 2017. The latest LLIS uses upgraded lighting detection processors and software to achieve higher efficiency and reliability.

4.4.1.1.4 Lightning Nowcasting System (LiNS)

LiNS provides C-G lightning strokes forecast to specialized users or corporate clients such as power company or cable car operator for assessing the needs for early preventive actions due to lightning threats. Forecasts of regional lightning strokes up to 2 hours ahead are generated using TREC and its ensemble motion vectors, semi-Lagrangian advection scheme and the temporal trend of the lightning intensity. Both graphical products and text alerts are distributed to the users in every 6 minutes interval. The alerting thresholds for individual clients are tailored towards their respective operation scenario. Direct output from LiNS was also used to support lighting alert service for the general public.

4.4.1.1.5 Satellite-based nowcasting

A nowcasting system on significant convection for the area (15°S – 45°N, 75°E – 145°E) was developed based on i) global lightning data; and ii) simulated radar reflectivity derived from brightness temperatures measured by geostationary satellite (Himawari-8) using a neural network algorithm. Extrapolation on the significant convection area was done using semi-Lagrangian advection. Verification suggest some skill with CSI over 0.6 for 0 to 6-hour accumulation.

4.4.1.2 Research performed in this field

4.4.1.2.1 SWIRLS

(a) Development of new features in Com-SWIRLS continued with new features including severe weather nowcasting module, support of radar raw data in different formats, and deployment using virtual appliance in Open Virtualization Format (OVF).
(b) Rainfall nowcast using deep learning with a novel technique was developed, namely the "trajectory gated recurrent unit" (TrajGRU) (Shi *et al.*, 2017), and was put into real-time trial for evaluation of performance.
(c) Satellite nowcast using EUMETSAT NWC SAF was made to generate trial real-time products of cloud mask, cloud type, cloud top height, convective initiation and rapid development

thunderstorms using Himawari-8 data. Developments of other satellite nowcast products such as cloud microphysics retrieval and convective rainfall rate were underway.

4.4.1.2.2 ATNS

A 3D tracking and extrapolation algorithm which is capable to produce a volumetric nowcasting output was being developed and under testing.

4.4.1.2.3 ATLAS

With enhanced lightning location information system with higher cloud-to-cloud detection efficiency, a study has been conduct to use cloud-to-cloud lightning as precursor of cloud-to-ground lightning alerts with encouraging results. The lightning sensors managed by HKO have been upgraded to newer models and new sensors have been installed at the Hong Kong International Airport and a nearby island to improve overall detection efficiency and accuracy. Benefit to the performance in ATLAS will be further studied.

4.4.1.2.4 Satellite-based nowcasting

Satellite nowcasting research on aviation hazards like turbulence and icing were also performed. An algorithm using multiple satellite channels to identify high-altitude icing crystals was developed (Ng et al. 2017). It uses random forest analysis technique to select the importance of channels or split windows. Preliminary verification suggest skill comparable to NCAR's Current Icing Product.

Besides, an algorithm using satellite atmospheric motion vectors and multiple satellite channels to identify turbulence region was being developed. Research on improving and enhancing the algorithms was still undergoing. For turbulence and icing, use of NWP simulated satellite imagery for producing a short term forecast will be tested.

4.4.2 Models for Very Short-range Forecasting Systems

4.4.2.1 In operation

4.4.2.1.1 Rainstorm Analysis and Prediction Integrated Data-processing System (RAPIDS)

RAPIDS provides QPF for the next 6 hours at 2 km resolution (Wong and Lai 2006, Wong *et al*. 2009). The system blends the outputs from SWIRLS and RAPIDS-NHM at 6-minute intervals with respective weightings determined from real-time verification of their precipitation predictions. Phase correction to correct spatial errors in the forecast precipitation field in RAPIDS-NHM was included. To correct the biases in rainfall intensity occasionally found in RAPIDS-NHM forecast, an intensity correction scheme, which is based on comparing cumulative distribution of rainfall intensity from SWIRLS rainfall analysis and RAPIDS-NHM short-term forecast, was also implemented. Using the time-lagged ensemble approach, probability forecasts of precipitation out to 6 hours are also generated by the system.

4.4.2.1.2 Six-hourly Short-term QPF System

The short-term QPF system facilitates forecaster's preparation of a 6-hourly rainfall forecast over Hong Kong out to 30 hours. Inputs included the QPF from SWIRLS, RAPIDS, RAPIDS-NHM, Meso-NHM, global models of JMA, ECMWF, NCEP, UKMO and ECMWF EPS. QPF from global models and Meso-NHM in heavy rain are calibrated with adaptive parameters for improved performance. A "blended" QPF derived as the average of constituent objective guidance was also provided.

4.4.2.2 Research performed in this field

4.4.2.2.1 Significant convection forecast

Testing of a trend-based blending of ATNS and RAPIDS-NHM simulated reflectivity produced promising results (Cheung, et al. 2014). The algorithm will be put to routine running to collect more cases to demonstrate its performance.

4.5 Specialized numerical predictions

4.5.1 Assimilation of specific data, analysis and initialization

4.5.1.1 In operation

4.5.1.1.1 SLOSH (Storm Surge Model)

The forecast position, minimum pressure and storm size of tropical cyclones at 6-hourly intervals from 48 hours before the time of closest approach to Hong Kong to 24 hours after are used as input to the SLOSH.

4.5.1.1.2 WAVEWATCH III (Wave Model)

Forecast surface wind data from JMA based on 00 and 12 UTC are used as input for the areas:
(1) 5 – 35 °N, 105 – 135 °E with grid resolution 1.25° × 1.25°,
(2) 21.25 – 22.5 °N, 113.75 – 115 °E with grid resolution 0.25° × 0.25°.

4.5.1.1.3 Accident Consequence Assessment System

The Accident Consequence Assessment System is used to assess the consequence of nuclear accident occurring at nearby nuclear power plants and to simulate the dispersion of radioactive materials from nuclear accident around the world. It consists of two systems, namely the RODOS (Real-time Online DecisiOn Support) system and FLEXPART (FLEXible PARTicle dispersion model).

The RODOS system, which was developed under the European Commission's Framework Programmes, has been adopted by HKO to assess the consequence of nuclear accident occurring at nuclear power plants within a few hundred kilometres from Hong Kong. A Java-based RODOS is installed and used operationally in HKO.

The RODOS system was configured and initialised with fixed background data including land use, nuclear reactor sites information, dose intervention levels for countermeasures, and source term library. The following data is assimilated during a model run:

(a) Source term of the radioactive release including quantity of different nuclides and their release durations.
(b) Meteorological data ingested from prognostic NWP data or via manual input. Prognostic model data at multiple levels for the area 18 – 28 °N, 108 – 118 °E from Meso-NHM based on 00 and 12 UTC runs are available regularly as input. Alternatively, the user can manually input the meteorological data including wind speed and direction, atmospheric stability condition and precipitation rate.

The FLEXPART (FLEXible PARTicle dispersion model), a Lagrangian transport and dispersion model for the simulation of long range atmospheric transport process of radioactive materials, was installed in HKO in 2016. The version of FLEXPART installed is 9.02. The following prognostic model data at multiple levels are retrieved regularly as input for driving the FLEXPART simulations:

(a) ECMWF 0.5-degree resolution data with global coverage,
(b) ECMWF 0.125-degree resolution data covering eastern Asia (18-30°N, 108-125°E), and
(c) NCEP GFS 1-degree resolution data with global coverage.

4.5.2 Specific models

4.5.2.1 In operation

4.5.2.1.1 SLOSH (Storm Surge Model)

A general description of SLOSH is summarised as follows:

Governing equation	Transport equations of motion
Prognostic variables	Horizontal components of transport, water height
Spatial grid and resolution	A curvilinear polar grid, from 1 km resolution near the centre of the Hong Kong Basin to 7 km in open sea, 83 × 146 grid points
Terrain and bathymetry	Land topography and water depth at sea points
Initialization	Initialization time proposed by Jelesnianski *et al.* (1992). Static height elevations due to storm's pressure drop at the initial time are added to the initial quiescent water level.
Boundary conditions	Scheme proposed by Jelesnianski *et al.* (1992) to cater for different water depths
Driving forces	Simplified model storm (Jelesnianski and Taylor, 1973)
Numerical technique	Explicit finite difference scheme

Further details can be found in Jelesnianski *et al.* (1992).

4.5.2.1.2 WAVEWATCH III (Wave Model)

A general description of WAVEWATCH III is summarised as follows. Nested model runs are implemented for the areas:
(1) 5 – 35 °N, 105 – 135 °E with grid resolution 1.25° × 1.25°,
(2) 21.25 – 22.5 °N, 113.75 – 115 °E with grid resolution 0.25° × 0.25°.

Governing equation	Spectral action density balance equation
Prognostic variables	Wave action density spectrum
Spatial grid and resolution	Mercator projection for the areas: (1) 5 – 35 °N, 105 – 135 °E, 1.25° × 1.25° resolution, 27 × 27 grid points including boundary data zone (2) 21.25 – 22.5 °N, 113.75 – 115 °E, 0.25° × 0.25° resolution, 8 × 8 grid points including boundary data zone
Bathymetry	Water depth at sea points (SRTM)
Intra-spectral grid	24 directions with 15° increment, 25 logarithmic frequency grid points
Initial conditions	Parametric fetch-limited JONSWAP spectrum
Boundary conditions	(1) For the large area run, initial conditions applied as constant boundary conditions (2) For the small area run, model outputs from the large area run are used as input boundary conditions
Source term (input and dissipation)	Tolman and Chalikov parameterization
Source term (nonlinear interactions)	Discrete interaction approximation
Source term (bottom friction)	JONSWAP parameterization
Propagation scheme	Ultimate Quickest scheme with averaging
Numerical technique	Fractional step method

Further details can be found in Tolman (2002).

4.5.2.1.3 Accident Consequence Assessment System

General descriptions of RODOS and FLEXPART are summarised as follows.

(a) RODOS

RODOS employs an atmospheric dispersion and deposition model called ATSTEP (Päsler-Sauer, J, 2007), which is a short range Gaussian puff model developed especially for quick simulations of accidental releases of airborne radioactive materials.

In ATSTEP, time-integrated elongated puffs are released. The transport of each elongated puff is achieved by two trajectories attached to both ends of the puff. These pairs of trajectories follow the inhomogeneous and variable 2-dimensional wind fields step by step. The elongated puffs perform all the necessary changes in position, shape, and orientation, such as stretching, rotations, shrinking, and sideways drift.

Because of the large size of the elongated puffs, the plume can be represented by a relatively small number of puffs. Correspondingly, the number of time steps needed for the simulation of the release and the transport is small. The elongated puff approximation reduces the computing time of the model. Less than 10 minutes is required for a complete dispersion and contamination prognosis with releases over several hours.

In ATSTEP, the following phenomena are considered in the modelling of atmospheric dispersion and the radiological situation: time dependent meteorology data, time dependent nuclide-group specific release rates, thermal energy and rise of the puffs released, dry and wet deposition and corresponding depletion of the cloud, gamma radiation from cloud and from ground, radioactive decay and build-up of daughter nuclides, and potential doses.

Regarding the spatial resolution of the results, for a range of 100 km from the release location, the innermost region has 20 × 20 grid cells with resolution of 0.25 × 0.25 km^2. Four more square frames containing cells with edge of double size, 4-fold, 8-fold and 16-fold size, surround this region. In the outermost cell, there are 50 × 50 grid cells each of 4 × 4 km^2.

(b) FLEXPART

FLEXPART is a Lagrangian particle dispersion model that simulates the long-range transport, diffusion, dry and wet deposition and radioactive decay of materials released from point, line, area or volume sources.

In FLEXPART, turbulent motions for wind components are parameterized assuming a Markov process based on the Langevin equation. Parameterized random velocities in the atmospheric boundary layer are calculated by surface sensible heat fluxes, surface stresses and other meteorological data. Due to the absence of suitable turbulence parameterizations above the atmospheric boundary layer, a constant vertical diffusivity 0.1 m^2/s is used in the stratosphere, whereas a horizontal diffusivity 50 m^2/s is used in the troposphere.

Radioactive decay is accounted for by reducing the particle mass according to the exponential decay equation with given half-life. Wet deposition also takes the form of an exponential decay process by using scavenging coefficients. Dry deposition is described by a deposition velocity. The deposition velocity of a gas is calculated with the resistance method. FLEXPART also includes a moist convective parameterization scheme to represent convective transport in a particle dispersion model.

Further details of FLEXPART can be found in Stohl et al. (2005).

4.5.2.2 Research performed in this field

The study on the application of JRODOS for nuclear accident consequence assessment in Hong Kong was completed and submitted for publication. Details of the results can be found in Leung et al. (2018).

WaveWatch III model was enhanced by increasing computational grid resolution and extending the model domain to cover North Indian Ocean and western North Pacific.

4.6 Extended range forecasts (ERF) (10 days to 30 days)

4.6.1 Models

4.6.1.1 Research performed in this field

A collaborative research project with a local power company was underway on the automatic daily max/min temperature forecasts for Day 10-14 based on EPS data with impact on power consumption management as the main thrust. The post-processing of the probability distribution function were also being considered.

4.7 Long range forecasts (LRF) (30 days up to two years)

4.7.1 In operation

HKO operates a suite of global-regional spectral climate models (2-tier) adapted from the Experimental Climate Prediction Center, USA. The model suite generates seasonal temperature and rainfall forecasts for Hong Kong, China. Products are made available to the general public via HKO's Internet website.

4.7.2 Research performed in this field

Various post-processing methods were developed to calibrate direct model output from major climate prediction centres to produce categorical and quantitative forecasts of monthly/seasonal temperature and rainfall. These calibrated forecasts generally perform better than the direct model output.

4.7.3 Operationally available products

Graphical representation of seasonal temperature and rainfall anomaly forecasts over southern China are available on HKO's website.

5 Verification of prognostic products

5.1 Annual verification summary

Verifications of forecasts generated by Meso-NHM are conducted on a routine basis. Forecast parameters including zonal and meridional winds, temperature, pressure/geopotential heights and relative humidity at a number of model levels are verified against respective model analyses and rawinsonde observations for the area 10 – 40°N, 95 – 135°E. The monthly verification results of Meso-NHM 12 UTC runs for 2017 are presented in Appendix I.

Verification of SLOSH outputs during the passage of tropical cyclones Merbok, Roke, Hato, Pakhar, Mawar and Khanum from June to October 2017 is shown in Appendix II.

Verification of prognostic products generated by WAVEWATCH III is shown in Appendix III.

6 Plans for the future (next 4 years)

6.1 Development of the GDPFS

6.1.1 HKO's dedicated website on RSMC for Nowcasting (https://rsmc.hko.gov.hk/nowcast/) will be enhanced with more nowcasting products for the Asian region. Support to RA II NMHSs in incorporating and using Com-SWIRLS for their rainstorm nowcasting operations will continue.

6.1.2 The HPC systems supporting operational NWP will be upgraded to a new CPU-based cluster with peak performance exceeding 200 TFLOPS.

6.1.3 An extended-domain limited-area prediction system based on WRF-ARW would be set up to support regional aviation hazard predictions under the Asian Aviation Meteorological Centre initiative.

6.1.4 An operational mesoscale ensemble prediction system initialised by ensemble-based assimilation technique such as EnKF would be set up to support impact-based and probabilistic forecasts of severe weather.

6.1.5 The 200-m resolution AVM would be extended to provide coverage for the Pearl River Estuary region which includes a number of major cities neighbouring Hong Kong.

6.1.6 The next-generation TIPS system will be developed on a GIS-enabled web platform to facilitate flexible, efficient and integrated display of various TC-related observations and forecast information.

6.2 Planned Research Activities in NWP, Nowcasting, Long-range Forecasting and Specialized Numerical Predictions

6.2.1 Planned Research Activities in NWP

(i) In collaboration with ECMWF under the SMUFF project (Seamless probabilistic MUlti-source Forecasting of heavy rainfall hazards for European Flood awareness; URL: http://fmispace.fmi.fi/index.php?id=smuff), an experimental system using pan European radar nowcast, namely ERICHA (European Rainfall-InduCed Hazard Assessment system), and ECMWF deterministic and EPS rainfall forecasts would be developed to integrate ERICHA radar nowcast with the adjusted QPFs from HRES and EPS for generating high-resolution seamless probabilistic rainfall prediction to support hazard and risk forecasting for the next 15 minutes to 5 days ahead.

(ii) The feasibility of convective-scale EPS and EnKF assimilation would be studied in conjunction with rapid-scan weather radar observations.

(iii) The impact of alternative radiative transfer models in computing simulated cloudy radiances would be studied.

(iv) Development of large-area aviation-specific forecast products for turbulence, icing and convection using in-house mesoscale model output

(v) Development of OCF to provide automatic weather forecasts for major cities and airports around the world.

(vi) A decision-support tool to facilitate efficient correction of digital weather forecasts by forecasters will be developed.

(vii) Probabilistic forecast products such as wind, pressure and precipitation in support of the development of forecast services for high-impact weather.

(viii) Model post-processing techniques and combining street-level observations with more advanced data quality control to generate automatic urban-scale forecast products.

(ix) Feasibility of computer fluid dynamics (CFD) modelling, including RANS and LES, for simulation of point source agent diffusion in urban envrionment in Hong Kong

(x) Use of machine-learning or deep-learning techniques in post-processing outputs from NWP models and EPSs to enhance the model objective guidance, in particular forecasts of genesis / rapid intensity change of tropical cyclones and other extreme weather events.

(xi) Enhancement of the SLOSH model domain by using latest LiDAR-based Digital Elevation Model and updated bathymetry data respectively provided by the CEDD (Civil Engineering and Development Department) and Marine Department.

(xii) Wavewatch III would be coupled with near shore wave model SWAN to generate high resolution wave products. Development of the Operational Marine Forecasting System to support the provision of marine meteorological services would be conducted.

6.2.2 Planned Research Activities in Nowcasting

(i) Enhancement of the operational SWIRLS with increased spatial resolution, more ensemble members, and incorporation of advanced nowcasting techniques.

(ii) Improvement of nowcasting techniques using machine learning and deep learning methods.

(iii) Developments in RSMC for Nowcasting to enhance real-time regional nowcasting products using radar and satellite and to provide a data sharing platform for exchange of nowcasting products.

(iv) Enhancement of Com-SWIRLS such as providing a collaborative development environment (e.g. Git-based platform) to promote software development among users.

(v) Development of nowcast-NWP blending system that seamlessly integrates radar, satellite, NWP deterministic models and EPS forecast products to improve forecasts of precipitation and significant convection.

6.2.3 Planned Research Activities in Long-range Forecasting

Efforts to investigate various statistical downscaling and post-processing techniques on WMO GPC digital model data and machine learning methods on pre-season atmospheric and oceanic indices to improve the skill of monthly/seasonal temperature and rainfall forecasts of Hong Kong would continue.

7 References

Arakawa, A. and W.H. Schubert, 1974: Interaction of a cumulus cloud ensemble with the large-scale environment, Part I. *J. Atmos. Sci.*, **31**: 674-701.

Beljaars, A., 1995: The parametrization of surface fluxes in large-scale models under free convection. *Quart. J. Roy. Meteor. Soc.*, **121**, 255-270.

Beljaars, A. C. M. and A. A. M. Holtslag, 1991: Flux parameterization and land surfaces in atmospheric models. *J. Appl. Meteor.*, **30**, 327-341.

Chan, P.K.Y, W.H. Leung and W.M. Ma, 2016: A Comparative Study of Atmospheric Dispersion Models. *30th Guangdong-Hong Kong-Macao Technical Seminar on Meteorological Technology,* 20 – 22 April 2016.

Chan, P.W. and K.K. Hon, 2015: Performance of super high resolution numerical weather prediction model in forecasting terrain-disrupted airflow at the Hong Kong International Airport: case studies. *Meteorol. Appl.,* **23**, 101-114.

Chan, P.W. and K.K. Hon, 2016: Observation and numerical simulation of terrain-Induced windshear at the Hong Kong International Airport in a planetary boundary layer without temperature inversions. Advances in Meteorology, vol. 2016, Article ID 1454513, 9 pages, 2016.

Chan, P.W., N.G. Wu, C.Z. Zhang, W.J. Deng and K.K. Hon, 2018: The first complete dropsonde observation of a tropical cyclone over the South China Sea by the Hong Kong Observatory. *Weather*, DOI: 10.1002/wea.3095.

Cheung, P. and C.C. Lam, 2011a: Development of significant convection forecast product and service for air traffic flow management in Hong Kong. *Second Aviation, Range and Aerospace Meteorology Special Symposium on Weather-Air Traffic Management Integration*, Seattle, WA, 23-27 January 2011.

Cheung, P. and C.C. Lam, 2011b: Objective calibrated wind speed and crosswind probabilistic forecasts for the Hong Kong International Airport. *Second Aviation, Range and Aerospace Meteorology Special Symposium on Weather-Air Traffic Management Integration*, Seattle, WA, 23-27 January 2011.

Cheung, P., P.W. Li and W.K. Wong, 2014: Blending of Extrapolated Radar Reflectivity with Simulated Reflectivity from NWP for a Seamless Significant Convection Forecast up to 6 Hours. *17th Conference on Aviation, Range, and Aerospace Meteorology*, Phoenix, Arizona, USA, 4-8 January 2015.

Chiu, Y.Y. and K.K. Hon, 2018: First studies on ensemble data assimilation over the South China coastal areas. *The 32nd Guangdong-Hong Kong-Macao Seminar on Meteorological Science and Technology*, Macau, 8-9 Jan 2018.

Donelan, M.A., B.K. Haus, N. Reul, W.J. Plant, M. Stiassnie, H.C. Graber, O.B. Brown and E.S. Saltzman, 2004: On the limiting aerodynamic roughness of the ocean in very strong winds. *Geophys. Res. Let.*, **31**, L18306.

Engel, C. and E. Ebert, 2007: Performance of hourly operational consensus forecasts (OCF) in the Australian region. *Wea. Forecasting*, **20**, 101-111.

Fairall, C.W., E.F. Bradley, J.E. Hare, A.A. Grachev and J.B. Edson, 2003: Bulk parameterization of air-sea fluxes: Updates and verification for the COARE algorithm. *J. Climate*, **16**, 571-591.

Hon, K.K., 2018: Simulated satellite imagery at sub-kilometre resolution by the Hong Kong Observatory. *Weather*, Vol. 73, No.5, 139-144, DOI:10.1002/wea.3100.

Hon, K.K., 2015: First studies on mesoscale ensemble prediction over the South China coastal areas. *29th Guangdong-Hong Kong-Macao Technical Seminar on Meteorological Technology,* 20 – 22 January 2015, Macau.

Hon, K.K. and P.W. Chan, 2017: Frequent-output sub-kilometric NWP models supporting enhanced runway throughput and performance-based navigation. WMO Aeronautical Meteorology Scientific Conference 2017, 6-10 November 2017, Toulouse, France.

Hon, K.K. and P.W. Chan, 2015: Sub-kilometre simulation of terrain-disrupted airflow associated with aircraft diversion at the Hong Kong International Airport. *33rd International Conference on Alpine Meteorology,* Innsbruck, Austria, 31 August – 4 September 2015.

Hon, W.Y. and K.K. Hon, 2016: First studies on mesoscale ensemble prediction of tropical cyclones over the South China coastal areas, 30th Guangdong-Hong Kong-Macau Seminar on Meteorological Technology, 20-22 April 2016, Guangzhou.

Jelesnianski, C.P., J. Chen and W.A. Shaffer, 1992: SLOSH Sea, Lake and Overland Surges from Hurricanes. *NOAA/NWS Technical Report NWS 48*.

Jelesnianski, C.P. and A.D. Taylor, 1973: A preliminary view of storm surges before and after storm modifications. *NOAA Technical Memorandum ERL WMPO-3*.

Kitagawa, H., 2000: Radiation process. *Report of Numerical Prediction Division*, **46**, 16-31 (in Japanese).

Leung, W.H., W.M. Ma, & Philip K.Y. Chan, 2018: Nuclear accident consequence assessment in Hong Kong using JRODOS, *Journal of Environmental Radioactivity,* **183**, 27-36.

Li, P.W. and D.S. Lau, 2008 : Development of a Lightning Nowcasting System for Hong Kong International Airport. *Presented in the 13th Conference on Aviation, Range and Aerospace Meteorology*, 20-24 January 2008, New Orleans, Louisiana, USA.

Li, P.W., 2009: Development of a thunderstorm nowcasting system for Hong Kong International Airport, AMS Aviation, Range, *Aerospace Meteorology Special Symposium on Weather-Air Traffic Management Integration*, Phoenix, Arizona, 11-15 Jan 2009.

Li, P.W., W.K. Wong, P. Cheung and H.Y. Yeung, 2014: An Overview of Nowcasting Development, Applications, and Services in the Hong Kong Observatory. *J. Meteo Res*, **28**, No. 5, 859-867, doi: 10.1007/s13351-014-4048-9.

Nakanishi, M. and H. Niino, 2004: Improvement of the Mellor-Yamada level 3 model with condensation physics: Its design and verification. *Boundary-Layer Meteorol.*, **112**, 1-31.

Ng, Y.L., H.F. Law, J.C.W. Lee, K.K. Hon, L.O. Li and P.W. Li, 2017: *Satellite Detection and Nowcasting High-altitude Ice Crystals*, WMO Aeronautical Meteorology Scientific Conference (AMSC-2017), MeteoFrance, Toulouse, France, 6 - 10 Nov 2017

Päsler-Sauer, J., 2007: Description of the Atmospheric Dispersion Model ATSTEP – Version RODOS PV 6.0 Final, RODOS(RA2)-TN(04)-03, Forschungszentrum Karlsruhe GmbH, Karlsruhe.

Saito, K., T. Fujita, Y. Yamada, J. Ishida, Y. Kumagai, K. Aranami, S. Ohmori, R. Nagasawa, S. Kumagai, C. Muroi, T. Kato, H. Eito and Y. Yamazaki, 2006: The operational JMA nonhydrostatic model. *Mon. Wea. Rev*., **134**, 1266-1298.

Shi, X.J., Z.R. Chen, H. Wang, D.Y. Yeung, W.K. Wong and W.C. Woo, 2015: Convolutional LSTM Network: A Machine Learning Approach for Precipitation Nowcasting, Advances in Neural Information Processing Systems **28**, arXiv:1506.04214 **[cs.CV]**

Shi, X.J., Z.H. Gao, L. Lausen, H. Wang, D.Y. Yeung, W.C. Woo, 2017: Deep Learning for Precipitation Nowcasting: A Benchmark and A New Model, Advances in Neural Information Processing Systems **30**, arXiv:1706.03458 **[cs.CV]**

Skamarock, W. C. and J. B. Klemp, 2008: A Time-Split Nonhydrostatic Atmospheric Model for Weather and Forecasting Applications. J. Comp. Phys., 227, 3465-3485.

Snyder, C. and F. Zhang, 2003: Assimilation of Simulated Doppler Radar Observations with an Ensemble Kalman Filter. *Mon. Wea. Rev.*, **131**, 1663-1677.

Song, M.K., L.S. Lee and K.K. Hon, 2017: Development of public weather services of the Hong Kong Observatory. Advances in Meteorological Science and Technology, **1**, 227-237.

Stohl, A., C. Forster, A. Frank, P. Seibert, and G. Wotawa, 2005: Technical Note : The Lagrangian particle dispersion model FLEXPART version 6.2. *Atmospheric Chemistry and Physics,* **5**, 2461-2474.

Tiedtke M., 1989: A comprehensive mass flux scheme for cumulus parameterization in large-scale models. *Mon. Wea. Rev.*, **117**, 1779-1800.

Tolman H.L., 2002: User manual and system documentation of WAVEWATCH-III version 2.22. *NOAA/NWS/NCEP/MMAB Technical Note 222*.

Troen I. and L. Mahrt, 1986: A simple model of the atmospheric boundary layer: Sensitivity to surface evaporation. *Boundary Layer Meteorl.*, **37**, 129-148.

Tsoi, T.S. and K.K. Hon, 2016: Experiments on cloud-resolving ensemble prediction of severe convection over the coast of Guangdong, 30th Guangdong-Hong Kong-Macau Seminar on Meteorological Technology, 20-22 April 2016, Guangzhou.

Woo, W.C., K.K. Li, Michael Bala, 2014: An Algorithm to Enhance Nowcast of Rainfall Brought by Tropical Cyclones Through Separation of Motions. *Tropical Cyclone Research and Review*, 3(2), 111-121.

Wong, W.K., 2011: Development of Operational Rapid Update Non-hydrostatic NWP and Data Assimilation Systems in the Hong Kong Observatory, *Technical Reports of the Meteorological Research Institute No. 65: "International Research for Prevention and Mitigation of Meteorological Disasters in Southeast Asia"*, p.87-100.

Wong, W.K. and E.S.T. Lai, 2006: RAPIDS – Operational Blending of Nowcast and NWP QPF. *presented in the 2nd International Symposium on Quantitative Precipitation Forecasting and Hydrology*, 4-8 June 2006, Boulder, Colorado, USA.

Wong, W.K., C.S. Lau and P.W. Chan, 2013: Aviation Model: a fine-scale numerical weather prediction system for aviation applications at the Hong Kong International Airport. *Advances in Meteorology*, Vol. 2013, Article ID 532475, 11 pages.

Wong W.K., M.K. Or, P.W. Chan and C.M. Cheng, 2011: Impact of Radar Retrieval Winds on Data Assimilation and Forecast of a Mesoscale Convective Storm using Non-Hydrostatic Model. *14th Conference on Mesoscale Process*, American Meteorological Society, Los Angeles, USA, 1-4 August 2011

Wong, W.K., S. Sumdin, and S.T. Lai, 2011: Development of Air-Sea Bulk Transfer Coefficients and Roughness Length in JMA Non-Hydrostatic Model, *Technical Reports of the Meteorological Research*

Institute No. 65: "International Research for Prevention and Mitigation of Meteorological Disasters in Southeast Asia", p.82-85.

Wong, W.K., S.M. Tse and P.W. Chan, 2013: Impacts of Reconnaissance Flight Data on Numerical Simulation of Tropical Cyclones over South China Sea, *Met. Application* DOI: 10.1002/met.1412.

Wong, W.K., L.H.Y. Yeung, Y.C. Wang and M. Chen, 2009: Towards the Blending of NWP with Nowcast — Operation Experience in B08FDP, *WMO Symposium on Nowcasting*, 30 Aug-4 Sep 2009, Whistler, B.C., Canada.

WOO, WC., W.K. Wong: Operational Application of Optical Flow Techniques to Radar-Based Rainfall Nowcasting, *Atmosphere* **2017**, *8*(3), 48; doi: 10.3390/atmos8030048

Yabu, S., S. Murai and H. Kitagawa, 2005: Clear sky radiation scheme. *Report of Numerical Prediction Division*, **51**, 53-64 (in Japanese).

Yeung, H.Y., C. Man, S.T. Chan and A. Seed, 2011: Application of radar-raingauge co-kriging to improve QPE and quality control of real-time rainfall data. *International Symposium on Weather Radar and Hydrology*, 18-21 April 2011, Exeter, U.K.

Appendix I — Summary of Verification of Prognostic Products Generated by Meso-NHM 12 UTC Runs for 2017 (Verification Area: 10 – 40 °N, 95 – 135 °E)

Table 1a. RMS error of mean sea level pressure against analysis (in m)

Hours	Jan	Feb	Mar	Apr	May	Jun	Jul	Aug	Sep	Oct	Nov	Dec	Average
24	1.5	1.5	1.7	1.4	1.2	1.3	1.5	1.4	1.3	1.5	1.6	1.5	1.5
72	2.9	2.6	2.4	1.9	1.8	1.8	1.9	2.2	2.4	2.7	2.3	2.8	2.3

Table 1b. RMS error of mean sea level pressure against observations (in m)

Hours	Jan	Feb	Mar	Apr	May	Jun	Jul	Aug	Sep	Oct	Nov	Dec	Average
24	1.5	1.6	1.6	1.3	1.2	1.3	1.6	1.5	1.4	1.4	1.4	1.5	1.4
72	3.1	2.9	2.6	1.9	1.8	1.7	1.7	2.0	2.2	2.7	2.3	2.7	2.3

Table 2a. RMS error of geopotential height at 500 hPa against analysis (in m)

Hours	Jan	Feb	Mar	Apr	May	Jun	Jul	Aug	Sep	Oct	Nov	Dec	Average
24	9.8	9.2	9.0	8.7	8.7	10.0	12.1	11.0	10.0	10.7	8.8	9.2	9.8
72	18.5	17.8	15.5	15.1	13.6	14.5	16.0	13.6	14.5	18.8	14.2	17.8	15.8

Table 2b. RMS error of geopotential height at 500 hPa against observations (in m)

Hours	Jan	Feb	Mar	Apr	May	Jun	Jul	Aug	Sep	Oct	Nov	Dec	Average
24	13.7	13.3	14.0	11.3	9.8	8.8	9.3	9.8	10.1	11.7	12.1	13.7	11.7
72	24.2	22.1	20.7	17.8	15.1	15.8	14.2	14.0	15.6	19.2	18.1	23.4	18.7

Table 3a. RMS error of vector wind error at 850 hPa against analysis (in m/s)

Hours	Jan	Feb	Mar	Apr	May	Jun	Jul	Aug	Sep	Oct	Nov	Dec	Average
24	3.3	3.2	3.3	3.4	3.4	3.4	3.5	3.4	3.6	3.8	3.4	3.4	3.4
72	4.8	4.6	4.8	4.7	4.8	5.0	5.3	5.3	5.9	5.9	4.7	5.1	5.1

Table 3b. RMS error of vector wind errors at 850 hPa against observations (in m/s)

Hours	Jan	Feb	Mar	Apr	May	Jun	Jul	Aug	Sep	Oct	Nov	Dec	Average
24	4.4	4.4	4.6	4.4	4.1	4.4	4.1	4.0	4.0	4.3	4.4	4.4	4.3
72	5.6	5.5	5.7	5.4	5.2	5.7	5.1	5.3	5.4	5.4	5.4	5.6	5.5

Table 4a. RMS error of vector wind errors at 250 hPa against analysis (in m/s)

Hours	Jan	Feb	Mar	Apr	May	Jun	Jul	Aug	Sep	Oct	Nov	Dec	Average
24	5.5	5.7	6.1	6.0	6.3	6.2	5.8	5.7	6.0	6.0	4.8	5.0	5.7
72	8.4	8.1	8.9	9.5	9.2	9.3	8.3	8.7	8.9	9.1	7.4	7.7	8.6

Table 4b. RMS error of vector wind errors at 250 hPa against observation (in m/s)

Hours	Jan	Feb	Mar	Apr	May	Jun	Jul	Aug	Sep	Oct	Nov	Dec	Average
24	9.9	10.1	10.1	9.1	8.4	8.4	6.3	6.5	7.3	7.3	8.5	9.2	8.5
72	11.4	11.4	11.6	11.3	10.5	10.0	8.1	9.5	9.5	9.5	9.8	10.3	10.3

Table 5a. RMS error of temperature at 850 hPa against analysis (in degree Celsius)

Hours	Jan	Feb	Mar	Apr	May	Jun	Jul	Aug	Sep	Oct	Nov	Dec	Average
24	1.6	1.6	1.6	1.3	1.2	1.2	1.1	1.1	1.1	1.3	1.5	1.6	1.4
72	2.8	2.5	2.2	1.9	1.8	1.6	1.4	1.6	1.6	2.0	2.2	2.7	2.0

Table 5b. RMS error of temperature at 850 hPa against observation (in degree Celsius)

Hours	Jan	Feb	Mar	Apr	May	Jun	Jul	Aug	Sep	Oct	Nov	Dec	Average
24	1.8	1.7	1.7	1.5	1.4	1.4	1.3	1.4	1.3	1.7	1.6	1.7	1.6
72	2.3	2.1	1.9	1.9	1.8	1.7	1.4	1.7	1.6	2.0	2.0	2.3	1.9

Table 6a. RMS error of relative humidity at 850 hPa against analysis (in %)

Hours	Jan	Feb	Mar	Apr	May	Jun	Jul	Aug	Sep	Oct	Nov	Dec	Average
24	16.4	16.7	16.3	15.6	14.3	13.7	12.5	13.0	13.6	14.7	15.5	16.0	14.9
72	22.1	22.6	22.9	21.2	20.0	17.2	15.6	16.9	18.3	20.2	20.8	22.1	20.0

Table 6b. RMS error of relative humidity at 850 hPa against observation (in %)

Hours	Jan	Feb	Mar	Apr	May	Jun	Jul	Aug	Sep	Oct	Nov	Dec	Average
24	12.8	13.5	12.5	13.3	12.9	12.6	12.4	12.5	12.3	13.8	12.5	12.7	12.8
72	14.0	14.3	13.7	14.2	14.2	13.4	13.1	13.6	13.1	14.8	13.8	13.7	13.8

Figure 1. RMS error of mean sea level pressure (in hPa) against analysis (solid lines) and observations (dotted lines) at selected forecast hours.

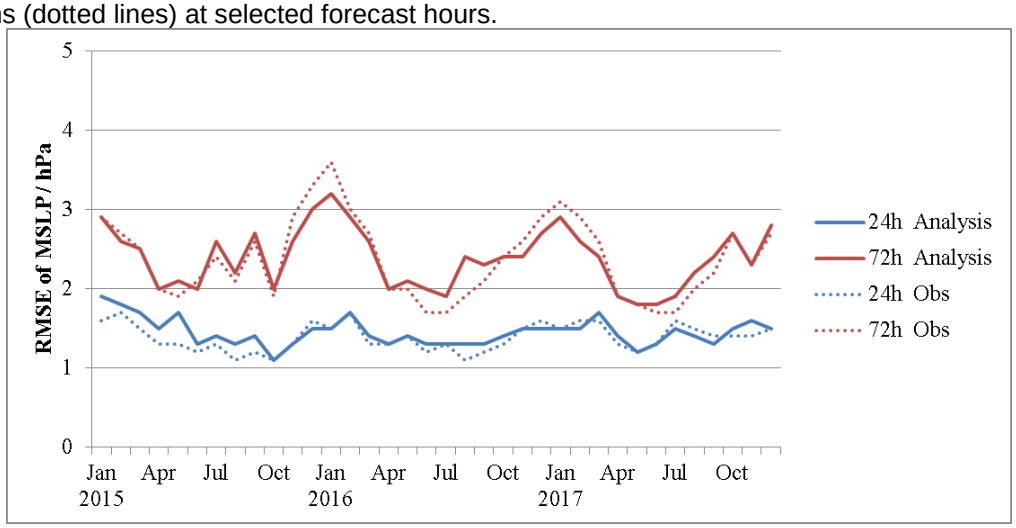

Figure 2. RMS error of geopotential height at 500 hPa (in m) against analysis (solid lines) and observations (dotted lines) at selected forecast hours.

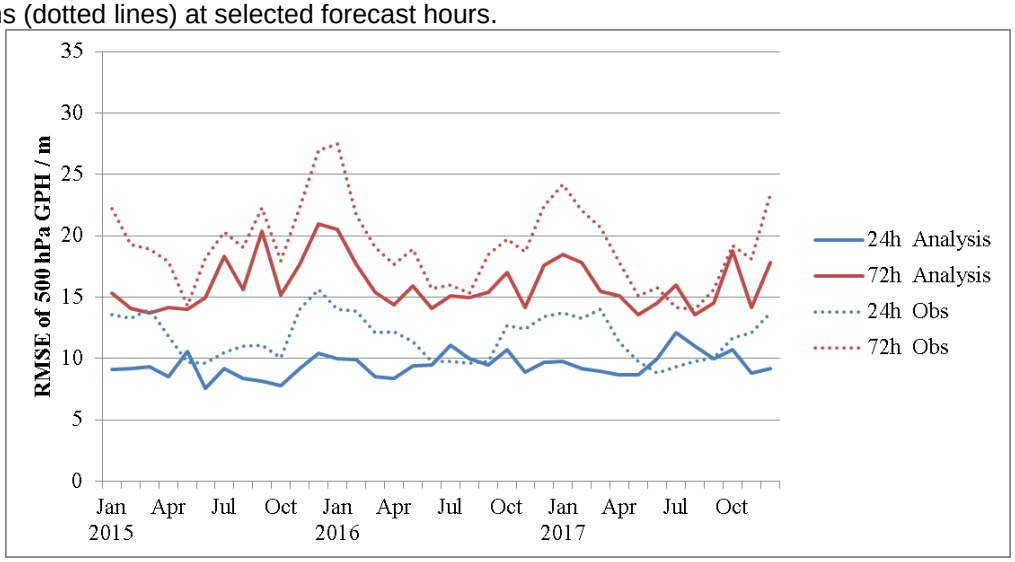

Figure 3. RMS error of vector wind at 850 hPa (in m/s) against analysis (solid lines) and observations (dotted lines) at selected forecast hours.

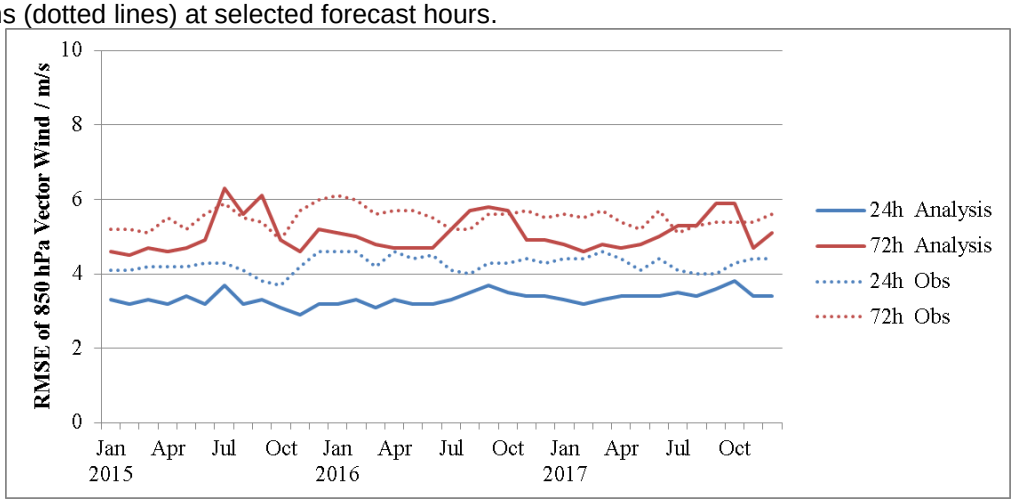

Figure 4. RMS error of vector wind at 250 hPa (in m/s) against analysis (solid lines) and observations (dotted lines) at selected forecast hours.

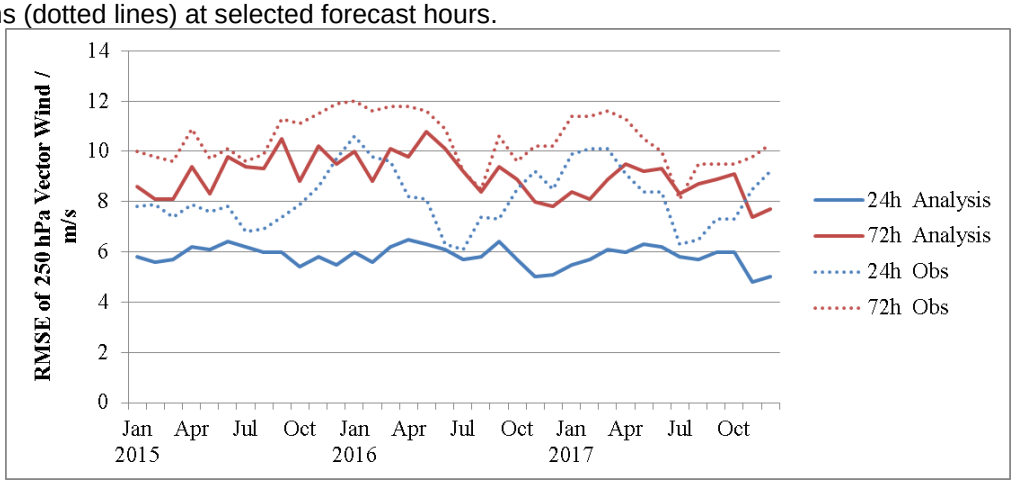

Figure 5. RMS error of temperature at 850 hPa (in degree Celsius) against analysis (solid lines) and observations (dotted lines) at selected forecast hours.

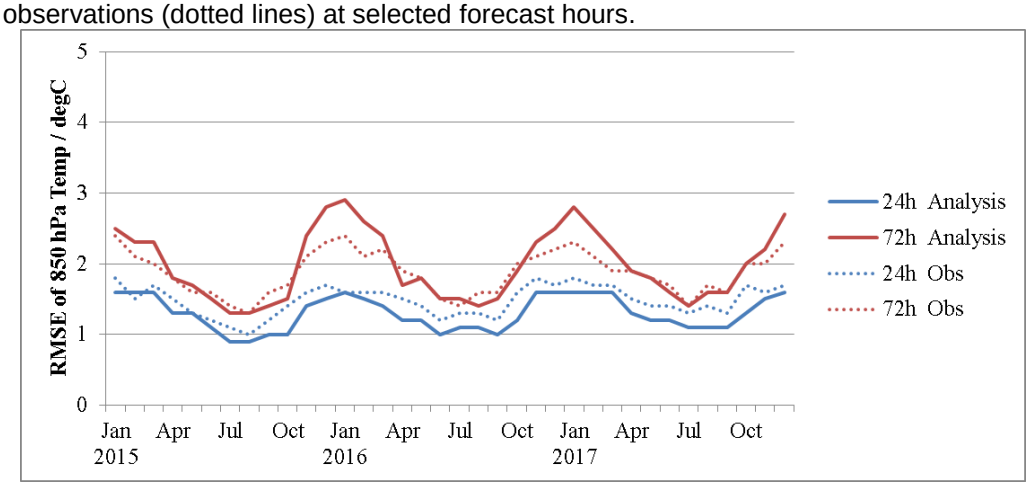

Figure 6. RMS error of relative humidity at 850 hPa (in %) against analysis (solid lines) and observations (dotted lines) at selected forecast hours.

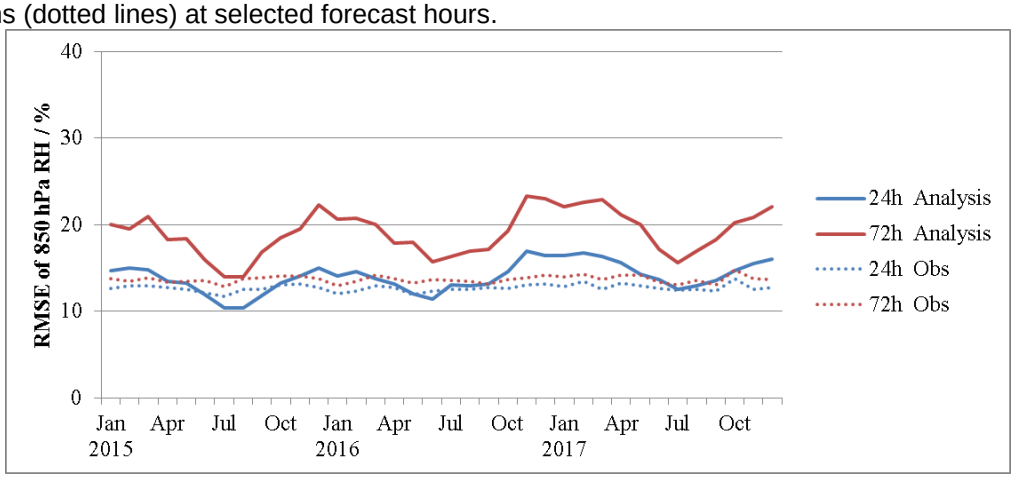

Appendix II – Summary of Verification of Prognostic Products Generated by SLOSH for 2017

Tropical cyclone	Year and Month	Observed maximum storm surge/sea level at Quarry Bay (m)	Predicted maximum storm surge/sea level at Quarry Bay (m)	SLOSH error (observed – Predicted storm surge/sea level (m)
Merbok	2017 Jun	0.24/2.35	0.46/2.37	-0.22/-0.02
Roke	2017 Jul	0.19/2.66	0.27/2.58	-0.08/0.08
Hato	2017 Aug	1.18/3.57	1.31/3.53	-0.13/0.04
Pakhar	2017 Aug	0.72/2.23	1.10/2.58	-0.38/-0.35
Mawar	2017 Sep	0.35/2.41	0.18/2.41	0.17/0.00
Khanun	2017 Oct	0.99/2.81	1.22/2.88	-0.23/-0.07

Appendix III – Summary of Verification of Prognostic Products Generated by WAVEWATCH III, 00 UTC and 12 UTC Runs for 2017

RMS error of 24-hour significant wave height forecast against observations (in m)

Jan-Mar	Apr-Jun	Jul-Sep	Oct-Dec	Year
1.4 (5081)	1.2 (3998)	1.2 (4025)	1.5 (5452)	1.3 (18556)

(Number of ship reports in brackets)